Synthesis and characterization of strongly fluorescent europium-doped calcium sulfide nanoparticles

Baoquan Sun,[a,c] Guangshun Yi,[a,c] Depu Chen,*[a,c] Yuxiang Zhou[b,c] and Jing Cheng[b,c]

[a]Department of Chemistry, Tsinghua University, Beijing 100084, P. R. China.
 E-mail: chendp@chem.tsinghua.edu.cn; Fax: (86) 10-62771149; Tel: (86) 10-62781691
[b]Department of Biological Science and Biotechnology, Tsinghua University, Beijing 100084,
 P. R. China
[c]Beijing National Biochip Research & Engineering Center, Beijing 100084, P. R. China

Nanometer-sized europium-doped calcium sulfide (CaS–Eu) particles were synthesized for the first time for potential use in bioassays, in particular, in biochip-based analysis. The CaS–Eu nanoparticles were prepared through a wet chemical process in ethanol. The average diameter of the nanoparticles was about 15 nm. They were characterized by UV–Vis spectrometry, scanning electron microscopy, X-ray diffraction, fluorescence spectroscopy and X-ray sequential fluorescence spectroscopy. Both electron paramagnetic resonance measurement and an extensive washing experiment revealed that the dopant atoms were internal ions dispersed throughout the whole CaS–Eu nanoparticles. Factors affecting the fluorescent properties of the nanoparticles were examined. It was found that the emission wavelength of the CaS–Eu nanoparticles could be altered by partial replacement of calcium with other alkaline earth metals such as magnesium, strontium and barium, and this makes the nanoparticles ideal for use as biochips where a multicolor-based bioassay is common.

Introduction

Rare earth element activated CaS phosphors have been widely studied since 1971[1,2] because of their potential as excellent fluorescent materials for efficient cathode-ray tube phosphors. The spectroscopic properties of pure and activated sulfides have been investigated and various applications of such materials in alloy semiconductors,[3] radiation dosimetry[4] and fast optically-stimulated luminescence imaging[5] have been attempted. For biological or biochemical reaction kinetics, it is preferred that the fluorescent materials employed are small in size and hence easily suspended in the reaction solution for a fast reaction. Fluorescent semiconductor nanocrystals (also known as quantum dots) have been reported as new bio-labeling materials for ultrasensitive detection of biological species such as antibodies, DNA and cells.[6–8] Nanoparticle labels have many advantages over organic fluorescent labels, such as their high sensitivity, low toxicity and large Stokes' shift, and therefore they have become more and more popular in various biological applications.

Europium activated alkaline earth element sulfides represent one class of the above-mentioned activated sulfides. Alkaline earth sulfides have a face-centered cubic structure, and are characterized by a high degree of ionicity.[9] These materials are in general strongly fluorescent under a wide range of excitation wavelengths, not amenable for photobleaching, and of high quantum yield. To the best of our knowledge, however, there is no report on the synthesis of nanometer-sized particles of europium-doped alkaline earth metal sulfides.

The rare earth doped CaS phosphors are usually prepared by sulfurizing calcium salts containing a rare earth activator in a hydrogen sulfide or a carbon disulfide atmosphere, which requires a long reaction time and consumes a great deal of energy.[10] They are usually produced from bulk materials at rather high temperature.[11] The particle size and fluorescent characteristics of the bulk phosphors greatly limit their applications in life sciences, disease diagnosis and drug discovery.[12,13] Wet chemical processes are practical approaches for nanoparticle synthesis since the size and crystallinity of the particle is easily controlled. The ease of control of particle size and crystallinity is important since the performance of the materials depends largely on the properties of the nanoparticles. The chemical growth control method has been used to prepare nanoparticles with a high degree of homogeneity at the molecular level. It would be ideal if the rare-earth doped alkaline earth sulfide nanoparticles could be prepared under convenient conditions. Unfortunately, it is impossible to obtain a calcium sulfide precipitate in aqueous solution because of its hydrolysis in water. More importantly, the fluorescent intensity of most europium doped metal sulfides (e.g. ZnS–Eu) prepared in water, is rather low.[14]

In this paper a novel wet chemical co-precipitation procedure was reported for the first time to prepare europium activated fluorescent nanoparticles. Ethanol was used as the solvent instead of water in order to decrease the hydrolysis of CaS and to enhance quantum yield of the nanoparticles. The relationship between fluorescent intensity and the concentration of europium in the sulfide was investigated. It was found that annealing time and temperature played an important role in determining the fluorescent properties of the nanoparticles. The optimal fluorescent nanoparticles were obtained after 2 h annealing in nitrogen at 700 °C. When calcium in the nanoparticles was partially replaced by magnesium, strontium and barium, some shifts in the fluorescent spectra were observed, indicating that the emission wavelength of the nanoparticles could be adjusted by changing the composition of alkali earth metals in the nanoparticles. The location of dopant atoms was determined by means of electron paramagnetic resonance (EPR) and an extensive washing experiment. The results reveal

DOI: 10.1039/b109352e

that the dopant atoms were incorporated in the lattice, rather than loosely bound to the surface of the nanoparticles.

Experimental section

Chemicals

All chemicals were of at least certified analytical grade. Alkali earth metal halides, $Na_2S \cdot 9H_2O$, $Eu(NO_3)_3 \cdot 6H_2O$ were obtained from Beijing Chemical Reagent Co. (Beijing, China). 1-Thioglycerol was acquired from Acros (Acros Organics, Geel, Belgium). All solutions were freshly prepared. A sulfide solution 0.0125 M was prepared by dissolving 0.3002 g (0.00125 mol) $Na_2S \cdot 9H_2O$ and 0.11 ml (1.15 mmol) of thioglycerol in 100 ml ethanol and sonicating for 30 min. Alkali earth metal halide solutions 0.025 M were prepared by dissolving appropriate amounts of the salts in 100 ml of ethanol. 0.01 M Eu stock solution was prepared by dissolving 0.0892 g $Eu(NO_3)_3 \cdot 6H_2O$ (0.2 mmol) in 20 ml of ethanol.

Apparatus

Transmission electron microscopic (TEM) images of the nanoparticles were acquired on an H-800 electron microscope (Hitachi Ltd., Tokyo, Japan) operating at 150 kV. Diluted nanoparticles suspended in ethanol were introduced onto a 50 Å thick carbon coated copper grid (400 mesh), and the particles were allowed to dry in air. The size distribution of the nanoparticles was determined using a BIC Zeta-plus zeta potential analyzer (Brookhaven Instruments Corp, Holtsville, NY). The powder was sonicated in ethanol for 20 min before measurement. X-Ray powder diffraction (XRD) experiments were carried out with a D8 Advance X-ray powder diffractometer (Bruker Instruments Inc, Billerica, MA) operating with a Cu anode at 45 kV and 30 mA. Element analysis of the nanoparticles was recorded on a XRF 1700 sequential fluorescence spectrometer (Shimazu Corp, Kyoto, Japan) operating at 4 kV and 80 mA. The concentration of europium in the CaS–Eu was determined by the Sciex FLAN 6000 quadrupole ICP-MS spectrometer (Perkin-Elmer Corp, Foster City, CA) using 2% HNO_3 to dissolve the solid nanoparticles. Fluorescent measurements were performed with a LS-50B luminescence spectrometer (Perkin-Elmer Corp, Foster City, CA) using the front surface accessory with equal quantity of nanoparticles every time. Absorption spectra were collected on a UV 2100S UV–Vis spectrometer (Shimazu Corp, Kyoto, Japan). Room temperature (9.77 GHz) electron paramagnetic resonance (EPR) spectra were obtained using a Bruker ESP 200D-SRC instrument (Bruker Instruments Inc., Billerica, MA). The magnetic field corrections were made with DPPH (1,1'-diphenyl-2-picrylhydrazyl) standard. The signals were averaged over 16–64 scans, depending on the signal quality.

Synthesis of the CaS–Eu nanoparticles

Methanol, ethanol, propanol and butanol have all been tested as the candidate solvents replacing water. It was found that ethanol was the best. The polarity of ethanol is perfect for dissolving the original reagents of $CaCl_2$, Na_2S and $Eu(NO_3)_3$ with the help of 1-thioglycerol. The synthesis of the CaS–Eu nanoparticles was performed as follows: 100 ml of $CaCl_2$ solution and different amounts of Eu solution were placed into a three-necked flask fitted with stoppers and valve. Nitrogen is used to protect the reaction system from forming calcium carbonate. The solution was deoxygenated with nitrogen for 15 min, followed by a swift injection of 100 ml of sulfide solution under vigorous stirring. The mixture was agitated at room temperature for 3 h. Particle growth occurred continuously at this stage via Ostwald ripening.

Size-selective precipitation was used to isolate the CaS–Eu nanoparticles from the mixture to harvest certain nanoparticles with narrow size distributions. 220 ml initial reaction mixture was concentrated down to approximately 50 ml in volume in a rotating evaporator, and tetrahydrofuran was added dropwise till turbidity occurred. The solution was stirred for 2 h, the first fraction of the nanoparticles was collected through centrifugation. The second and third fractions were isolated in a similar manner by adding more and more tetrahydrofuran and through centrifugation. The mole yield of nanoparticles precipitated is about 62.2% with respect to the calcium ions. In this way, the nanoparticles of different sizes with narrow size distributions were prepared. The diameter of the nanoparticles of the first fraction was the largest; and that of the third fraction the smallest. All precipitates obtained were washed with 0.01 M K_2CO_3 95% ethanol (pH 11) three times and then anhydrous ethanol once. Then they were heated in the anhydrous ethanol at 70 °C for four hours and dried under vacuum to remove any residual ethanol. Finally they were annealed under a nitrogen atmosphere.

Results and discussion

Synthesis of the CaS–Eu nanoparticles

Bulk phosphors of CaS–Eu were readily prepared by sintering a mixture of calcium salt and sodium sulfide at high temperature. However, the required preparation of CaS–Eu nanoparticles should include production of particles with both a narrow size distribution and a strong fluorescent intensity. Synthesis of nearly monodispersed nanoparticles was achieved by using supersaturation for sudden nucleation and subsequent growth.[15] Calcium sulfide nanoparticles were difficult to prepare in aqueous solution because of their hydrolysis in water. Therefore ethanol was chosen as candidate solvent and 1-thioglycerol was used to stabilize the sulfide particles in the solvent. It has been reported that 1-thioglycerol is adsorbed on the surface of the slide particles,[16,17] which can stabilize nanometer sized cadmium sulfide in dimethylformamide. This prompted us to use 1-thioglycerol as a stabilizer for CaS–Eu in ethanol.

In addition the europium ion is stable and the CaS–Eu nanoparticles formed had very low solubility in ethanol. The XRD spectra of the nanoparticles obtained from ethanol and water are shown in Fig. 1. The precipitate obtained in aqueous solution is europium oxide and not the sulfide. Only in ethanol, were the CaS–Eu nanoparticles formed. The XRD spectra of as-prepared CaS–Eu showed a match with the diffraction pattern available in the PDF-2.01database (77-2011). The
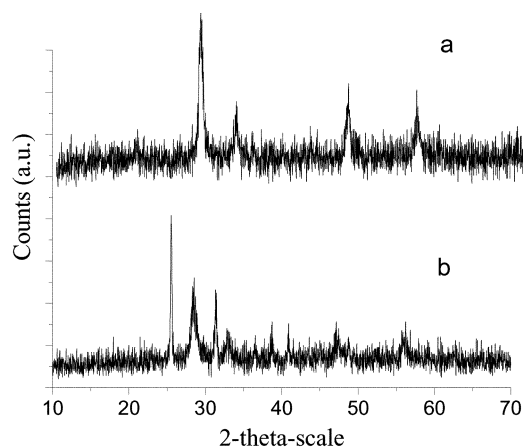

Fig. 1 Powder X-ray diffraction patterns of (a) the cubic sulfide nanoparticles obtained from ethanol annealed at 700 °C; (b) the cubic europium oxide obtained from water annealed at 700 °C.

CaS–Eu sample is obtained in the cubic form, with lattice parameter $a = 5.686$.

Size distribution of the nanoparticles

Superfluous sulfide ion was abruptly injected into solution, which led to rapid formation of relatively large amounts of nanoparticles. The initial concentrations of the reagents, stirring rate and reaction temperature all affected the size and size distribution of the nanoparticles. Nucleation takes place rapidly after injection and continues until the monomer concentration drops below a critical threshold. The size of the nanoparticles was averaged during the particle growth period as the smaller particles grow faster than the larger ones. When the monomer concentration is depleted as a result of the particle growth, some smaller nanoparticles shrink and eventually disappear, while larger ones tend to grow bigger in the solution. Nanoparticles with a relatively narrow size distribution could be obtained with careful operation. The nanoparticles prepared were steadily suspended in ethanol for many days without any notable changes. Moreover, nanoparticles of different sizes were obtained by the size-selective precipitation method as mentioned above. UV–Vis absorption spectra of the crude colloidal solution, Sample m (without separation), and Sample a, b, and c obtained after three successive size-selective isolations from sample m, are shown in Fig. 2. Sample m represents a mixture of the CaS–Eu nanoparticles with a wide size distribution. The diameter of the nanoparticles gradually decreased from Sample a to Sample c. Absorption spectra in the range of 200–250 nm and 250–320 nm were found to shift gradually to longer wavelength according to the order of sample a, b and c. This change may relate to the size effect, as suggested in the literature.[18] Compared with the bulk materials, more europium ions lie at the surface of solids. The smaller the particle, the more ions surround the particles. The different absorption characters observed with different particle size can be related to the different contribution of the europium ions to absorption character between interior and exterior ions. A TEM image of Sample c is shown in Fig. 3. The diameter of the nanoparticles was about 15 nm, and the size distribution was almost monodispersed (Fig. 4) within ± 3 nm range. The fluorescent life time of the nanoparticles is about 1.5 ms, whereas that of the organic fluorescent dye is only dozens of nanoseconds. The energy efficiency of the nanoparticles was about 60% of that of the standard red phosphor, Y_2O_2S–Eu. On the other hand, the energy efficiency of bulk CaS–Eu materials was only 20%.

Fig. 3 The TEM image of the CaS–Eu nanoparticles containing 0.85% europium. Sample shown was from the third fraction and annealed at 700 °C.

Fig. 4 Particle size distribution of the CaS–Eu nanoparticles containing 0.85% europium. The sample was from the third fraction and annealed at 700 °C.

Effect of other alkaline earth metals on the fluorescent properties of the nanoparticles

The wavelength of the emission of the nanoparticles can be adjusted *via* the addition of other alkaline earth metals such as magnesium, strontium and barium to the reaction mixture. The emission spectra of the nanoparticles containing different alkaline earth metals are presented in Fig. 5. Different amounts of Mg, Sr and Ba were added into the nanoparticles, and the molar ratios of replacement elements to calcium in the nanoparticles were 3.1%, 7.0% and 1.6% for Mg, Sr and Ba, respectively, according to the element analysis. It is seen from Fig. 5 that barium and strontium make the excitation and emission spectra shift to the blue area; on the other hand, magnesium makes the spectrum shift to the red region. The ionic radius of Sr^{2+} is close to that of Ca^{2+}, hence Ca^{2+} in the
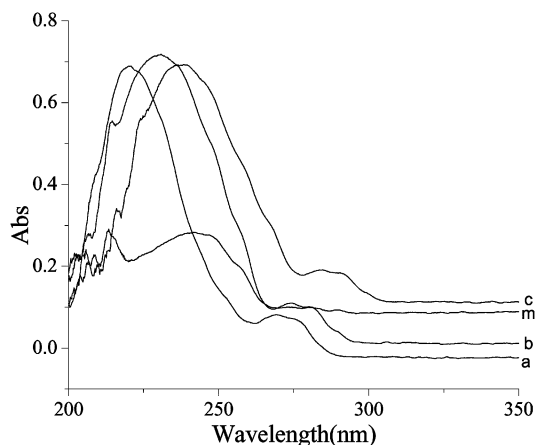

Fig. 2 UV–Vis absorption spectra of different fractions of the CaS–Eu nanoparticles. Sample m was the original reaction mixture before fractionation, Sample a, b and c were the first, second and third fraction, respectively.
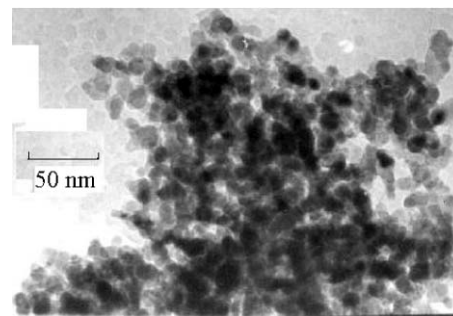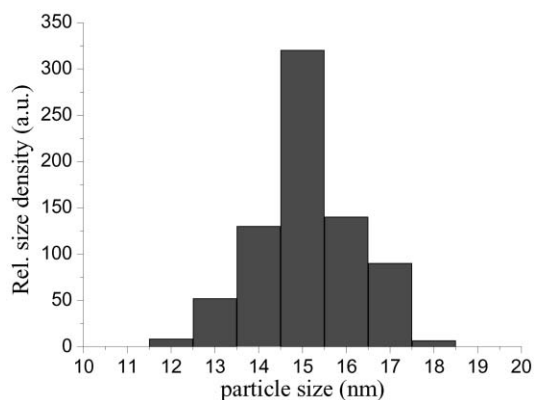

a: $Ca_xSr_{1-x}S$:Eu
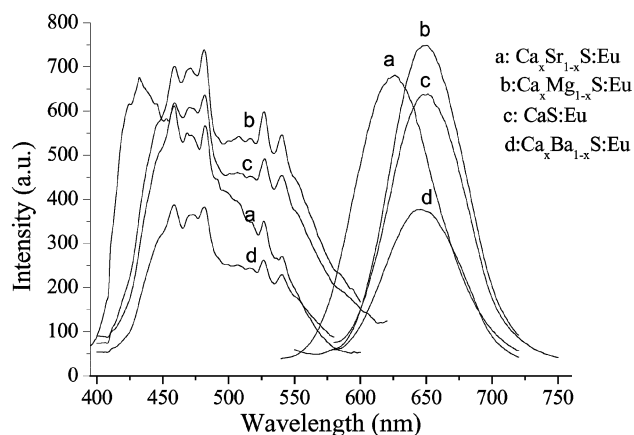b: $Ca_xMg_{1-x}S$:Eu
c: CaS:Eu
d: $Ca_xBa_{1-x}S$:Eu

Fig. 5 The fluorescent spectra of the CaS–Eu nanoparticles containing different alkaline earth metals. Samples were annealed at 700 °C.

nanoparticles might easily be replaced by Sr^{2+}. Of all alkaline earth metals tested strontium had the most obvious affect on the emission wavelength of the nanoparticles.

Effect of the europium concentration on the fluorescent intensity

The emission spectra of the nanoparticles consisted of a single emission band originating from the intraionic transitions in the europium ion.[18] The dependence of the fluorescent intensity of the nanoparticles on the concentration of europium is illustrated in Fig. 6. It can be seen clearly that the fluorescent intensity of the nanoparticles changes with the europium content. The highest quantum yield of the nanoparticles was obtained at a europium concentration of approximately 0.85 mol%. Lower or higher europium contents could result in a substantial decrease in fluorescent intensity. With the increment of the concentration of activator ion, the fluorescent center is increased and the fluorescent intensity enhanced. When the concentration of the activated element was higher than a threshold concentration, any further increase in concentration decreased the fluorescent intensity. It has been reported that concentration quenching of the fluorescence of rare earth metals such as Eu, Gd and Tb compounds could take place in the case of superfluous doping rare earth ions. When the concentration of rare earth metal is higher than a certain threshold, the energy migration of neighboring rare earth ions would kill the fluorescence.[19]

Effect of annealing temperature and time on the fluorescent properties of the nanoparticles

The nanoparticles prepared in the wet chemical procedure had very low fluorescent intensity before annealing because of their extremely poor crystallinity. The strongest fluorescent intensity was achieved by annealing the nanoparticles at 700 °C in nitrogen. The temperature to anneal the nanoparticles was lower than that required in the preparation of bulk materials (1100 °C). The results of temperature dependency of the fluorescent intensity are shown in Fig. 7. From Fig. 7 it is shown that the fluorescent intensity increased almost linearly with the increase of annealing temperature and a maximum fluorescent intensity was obtained at 700 °C. Further increase in annealing temperature had some detrimental effect on the fluorescent intensity. XRD data of the nanoparticles annealed in nitrogen shows that some sulfide in the nanoparticles was oxidized into sulfate at temperatures higher than 700 °C, weakening the emission intensity. In addition, the annealing time played an important role in determining the fluorescent intensity of the nanoparticles, as presented in Fig. 8. The optimal annealing time is 2 h. Therefore it is recommended that for the synthesis of CaS–Eu nanoparticles with the highest (quantum yield) fluorescent intensity, the optimal annealing condition is at 700 °C for 2 h.
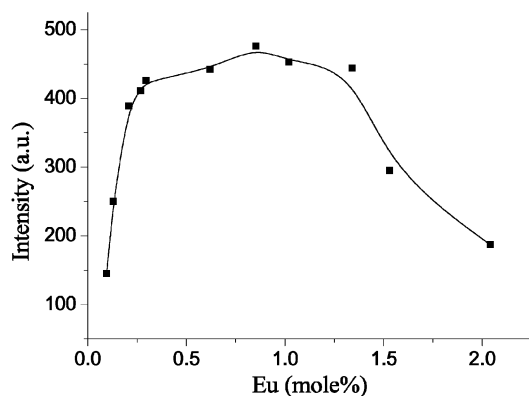

Fig. 6 Dependence of emission intensity of the CaS–Eu nanoparticles on the concentration of europium.
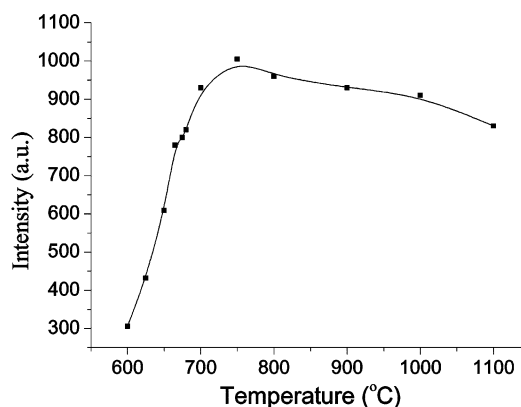

Fig. 7 Dependence of fluorescent intensity of the CaS–Eu nanoparticles containing 0.85% europium on annealing temperature in nitrogen.
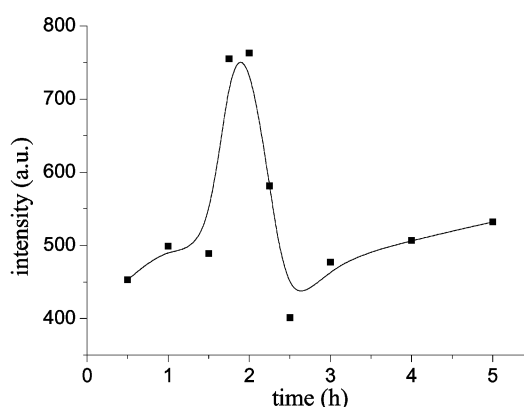

Fig. 8 Dependence of fluorescent intensity of the CaS–Eu nanoparticles containing 0.85% europium on annealing time at 700 °C in nitrogen.

Dopant europium atoms in calcium sulfide nanoparticles

Recently Bawendi and co-workers[20] have studied in detail the binding location of dopant atom Mn in doping CdSe nanoparticles. According to the report, if the EPR hyperfine splitting of the Mn in CdSe nanoparticles was bigger than that of bulk materials, it could be concluded that the dopant atoms reside near the more ionic surface layer of the nanoparticles. Therefore, we have used EPR spectroscopy and an extensive washing experiment to explore the europium distribution in CaS–Eu nanoparticles.

Fig. 9 displays the EPR spectrum of the CaS–Eu nanoparticles. The multicomponent character of europium spectra was
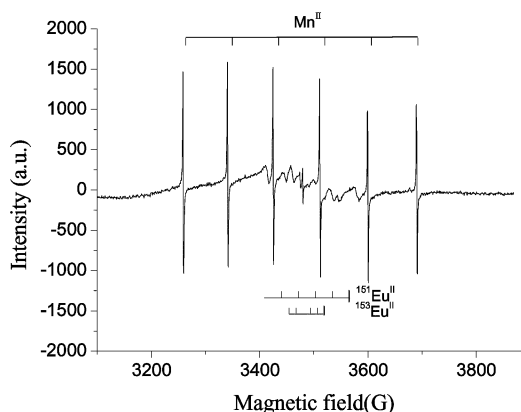

Fig. 9 EPR spectrum (300 K) of CaS–Eu nanoparticles after annealed at 700 °C. Microwave frequency $\upsilon = 9.77$ GHz, microwave power $P = 10$ mW.

due to the existence of two isotopes (^{151}Eu and ^{153}Eu, respectively). The two sets of six line pattern were the signature of europium hyperfine splitting (nuclear spin $I = 5/2$). Examination of the hyperfine splitting in the europium doped sulfide provides information on the bonding characteristics of the dopant's local environment. In our experiment, the hyperfine coupling constants for the two europium isotopes in CaS–Eu nanoparticles were as follows: $^{151}A = 32.58$ G and $^{153}A = 14.06$ G. On the other hand, the hyperfine coupling constants for the two europium isotopes in CaS–Eu bulk materials were reported as $^{151}A = 3.27$ mT (32.7 G) and $^{153}A = 1.44$ mT (14.4 G).[21] The hyperfine splitting value of CaS–Eu nanoparticles compared well with the known corresponding bulk system. It was shown that the europium bonding environment of CaS–Eu nanoparticles was similar to that of bulk materials. In bulk materials, europium ions substitute calcium ions in the cubic symmetry lattice.[18,22] Therefore it follows that the europium ions reside as internal ions substituting calcium ions in the CaS lattice.

To verify further the europium location in the nanoparticles, a washing of the nanoparticles experiment was carried out. The saturated ethylenediaminetetraacetic acid disodium (EDTA) ethanol solvent was used to wash the CaS–Eu nanoparticles extensively. After ligand exchange with EDTA, the quantity of europium atoms in ethanol and that left in the nanoparticles were determined by ICP-MS. The mol ratio of europium in ethanol to that left in the nanoparticles was 3.5 : 96.5. This indicated that only a limited amount of europium is dispersed on the surface of the nanoparticles. It may be concluded that the dopant europium ions were internal ions.

The oxidation state of europium in CaS–Eu nanoparticles could be Eu^{2+}. It is reported in the literature that the oxidation state of europium in CaS–Eu bulk materials was divalent.[21,23] Because there is no single electron in Eu^{3+}, Eu^{3+} doped samples do not give an EPR spectrum. Only Eu^{2+} ($J \neq 0$) could be detected by EPR. Moreover, the orbital moment of Eu^{2+} is $L = 0$, its relaxation time T_1 is relatively long, so Eu^{2+} is readily detected at 300 K. In our experiment, when the CaS–Eu nanoparticles were not annealed, there was no EPR signal from the europium element. And after annealing, the fine-structure EPR spectrum was observed, as shown in Fig. 9. It may be concluded that divalent europium ions exist in the luminescent nanoparticles. In the annealing process, trivalent europium ions are reduced to divalent ions.

Conclusion

A novel wet chemical co-precipitation procedure was reported to synthesize CaS–Eu nanoparticles. Nanoparticles of *ca.* 15 nm in diameter with relatively narrow size distribution were achieved through the reported process. The fluorescent properties of the nanoparticles depended on three main factors: the amounts of europium and other alkaline earth metals presented in the nanoparticles, the annealing temperature and the annealing time. Both the EPR hyperfine splitting and the extensive washing experiments show that the dopant europium atoms were distributed throughout the calcium sulfide lattice.

The range of the excitation wavelengths (420–560 nm) allows the wavelength of commercially available lasers or other lighting source to be easily matched to the fluorescent label. The fluorescence lifetime (ms) observed with the synthesized nanoparticles is much longer than that of the organic dyes (ns). These properties of the nanoparticles suggest that they could potentially be the new class of promising fluorescent labels for use in life sciences, disease diagnosis and drug discovery.

References

1 W. Lehmann, *J. Lumin.*, 1972, **5**, 87.
2 W. Lehmann and F. M. Ryan, *J. Electrochem. Soc.*, 1971, **118**, 477.
3 M. A. Tamor, L. C. Davis and H. Holloway, *Phys. Rev. B: Condens. Matter*, 1983, **28**, 3320.
4 R. P. Rao and D. R. Rao, *Health Phys.*, 1983, **45**, 1001.
5 J. Gasiot, P. Braunlich and J. P. Fillard, *Appl. Phys. Lett.*, 1982, **40**, 376.
6 M. Bruchez, M. Moronne, P. Gin, S. Weiss and A. P. Alivisatos, *Science*, 1998, **281**, 2013.
7 K. Kato and F. Okamoto, *Jpn. J. Appl. Phys. Part 1*, 1983, **22**, 76.
8 B. Q. Sun, W. Z. Xie, G. S. Yi, D. P. Chen, Y. X. Zhou and J. Cheng, *J. Immunol. Methods*, 2001, **249**, 85.
9 J. C. Philips, *Rev. Mod. Phys.*, 1970, **42**, 317.
10 W. C. W. Chan and S. M. Nie, *Science*, 1998, **281**, 2016.
11 M. Phamthi and G. Ravaux, *J. Electrochem. Soc.*, 1991, **138**, 1103.
12 H. B. Beverloo, A. Vanschadewijk, H. Zijlmans and H. J. Tanke, *Anal. Biochem.*, 1992, **203**, 326.
13 J. Hampl, M. Hall, N. A. Mufti, Y. M. M. Yao, D. B. Macqueen, W. H. Wright and D. E. Cooper, *Anal. Biochem.*, 2001, **288**, 176.
14 L. D. Sun, C. H. Yan, C. H. Liu, C. S. Liao, D. Li and J. Q. Yu, *J. Alloys Compd.*, 1998, **27**, 234.
15 X. G. Peng, J. Wickham and A. P. Alivisatos, *J. Am. Chem. Soc.*, 1998, **120**, 5343.
16 A. Chemseddine and H. Weller, *Ber. Bunsen-Ges. Phys. Chem.*, 1993, **97**, 636.
17 T. Vossmeyer, L. Katsikas, M. Giersig, I. G. Popovic, K. Diesner, A. Chemseddine, A. Eychmuller and H. Weller, *J. Phys. Chem.*, 1994, **98**, 7665.
18 Y. Nakao, *J. Phys. Soc. Jpn.*, 1980, **48**, 534.
19 G. Blasse and B. C. Grabmaier, *Luminescent Materials*, Springer-Verlag, Berlin, 1994.
20 F. V. Mikulec, M. Kuno, M. Bennati, D. A. Hall, R. G. Griffin and M. G. Bawendi, *J. Am. Chem. Soc.*, 2000, **122**, 2532.
21 D. Caurant, D. Gourier, N. Demoncy, I. Ronot and M. Phamthi, *J. Appl. Phys.*, 1995, **78**, 876.
22 M. Phamthi, N. Ruelle, E. Tronc, D. Simons and D. Vivien, *Jpn. J. Appl. Phys. Part 1*, 1994, **33**, 1876.
23 Y. Tamura and A. Shibukawa, *Jpn. J. Appl. Phys. Part 1*, 1993, **32**, 3187.